# SANDIA REPORT

SAND98–0251 • UC–704
Unlimited Release
Printed January 1998

# Sol-Gel Preservation of Mankind's Cultural Heritage in Objects Constructed of Stone

C. Jeffrey Brinker, Carol S. Ashley, Alan S. Sellinger, Randall T. Cygan, Kathryn L. Nagy, Roger Assink, Todd Alam, Sudeep Rao, S. Prabakar, Cathy S. Scotto

Prepared by
Sandia National Laboratories
Albuquerque, New Mexico 87185 and Livermore, California 94550

Sandia is a multiprogram laboratory operated by Sandia Corporation, a Lockheed Martin Company, for the United States Department of Energy under Contract DE-AC04-94AL85000.



Sandia National Laboratories

SAND98-0251 Distribution
Unlimited Release Category UC-704
Printed January 1998

# Sol-Gel Preservation of Mankind's Cultural Heritage in Objects Constructed of Stone

C. Jeffrey Brinker, Carol S. Ashley*, and Alan S. Sellinger
Advanced Materials Laboratory/Direct Fabrication Technologies Department

Randall T. Cygan and Kathryn L. Nagy
Geochemistry Department

Roger Assink and Todd Alam
Materials Aging and Reliability Department

Sandia National Laboratories
PO Box 5800
Albuquerque, New Mexico 87185-1349

Sudeep Rao[1] and S. Prabakar[2]
UNM/SNL Advanced Materials Laboratory
[1]Department of Civil Engineering
[2]Department of Chemical & Nuclear Engineering
University of New Mexico
Albuquerque, New Mexico 87131

Cathy S. Scotto
Optical Sciences Division
Naval Research Laboratory
Washington, D.C. 20375-5338

## Abstract

Monuments, buildings, and works of art constructed of carbonate-based stone (calcite, e.g., limestone and marble) are subject to deterioration resulting from the effects of environmental exposure, granular disintegration, freeze/thaw cycles, and salt recrystallization. This damage can potentially be reversed by the use of mineral-specific chemical passivants and consolidants that prevent hydrolytic attack and mechanical weakening. Our treatment strategy combined the use of calcite coupling molecules to *passivate* the surfaces against new weathering with alkoxysilane strengthening or *consolidating* layers to arrest physical deterioration. We report on the effectiveness of passivating agents designed through a combined approach of modeling their adhesive and passivating properties using computations at the molecular scale and testing those properties using simulated leaching tests, microscopic evaluation, and characterization of mechanical strength. The experimental results indicate that there may be a threshold binding energy for the passivant above which the dissolution rate of calcite is actually enhanced. Passivant/consolidant treatments were identified which showed substantial reductions in the leach rate of calcite exposed to simulated acid rain conditions.

* Author to whom correspondence should be addressed: csashle@sandia.gov

## Acknowledgments

The authors gratefully acknowledge valuable collaborations with our colleagues in the conservation community. Discussions between Dr. George Segan Wheeler, Metropolitan Museum of Art, and Jeff Brinker provided the original inspiration for this project. Dr. Wheeler also generously supplied limestone cores and participated in many helpful discussions on the art and science of conservation. Drs. William Ginell and Eric Doehne, The Getty Conservation Institute, provided insight into the needs of conservators and the application of Environmental Scanning Electron Microscopy (E-SEM) to art conservation.

The authors also wish to thank Howard Anderson for performing the calcite leaching experiments and Dr. Alan Wagner of the Lovelace Research Foundation for collaboration on the MRI analysis.

# Contents

## Figures



## Tables

# Introduction

**Objective.** This report summarizes the results of a three year Laboratory Directed Research and Development (LDRD) project aimed at the development of a protective process for the treatment of calcite based minerals (marble and limestone). Although moderately effective conservation treatments exist for sandstones (silicates), no proven system exists for limestones (carbonates). Based on Sandia's broad experience in sol-gel derived materials, geochemistry, and molecular modeling and simulation, a multidisciplinary approach was utilized to develop a mineral-specific, engineered protection strategy for calcite-based objects and structures. The protection treatment was designed to both *passivate* mineral surfaces against new weathering and strengthen or *consolidate* the existing weathered state to arrest granular disintegration and mitigate deterioration due to freeze/thaw cycles and salt crystallization.

**Historical Perspective.** Our cultural heritage, as reflected in artifacts and works of art, is being lost at an alarming rate due to the ravages of nature and abuse by mankind. Since the industrial revolution, chemical by-products of man's technological advances have caused the deterioration of many of our most precious cultural treasures.[1-3] Most vulnerable are sandstone and limestone objects – buildings, monuments, and sculpture – that are subjected to outdoor environments in industrialized or urban settings. Sandstones (quartz) are generally resistant to the action of acid rain because of the natural chemical resistance of silicate minerals. Works of limestone and marble, composed of the mineral calcite, are particularly sensitive to erosion from environmental factors. Acid rain and salt crystallization in combination with natural freezing and thawing of water, wetting and drying, and biodeterioration have caused extensive degradation of irreplaceable art objects and architectural works constructed of stone exposed to outdoor environments.[4] The consequences of these deterioration processes – granular disintegration, scaling, spalling, and flaking – have disfigured sculpture to unrecognizable states and have led to the widespread and costly problem of erosion of buildings and artworks. Similar processes are responsible for the degradation of roadways, bridges, and other reinforced concrete structures. The costs attributed to atmospheric corrosion and corrosion prevention approach 3% of the Gross National Product of industrialized countries.[5]

Historically, a variety of organic and inorganic surface treatments have been used to repel water and strengthen the matrix of stone structures. These treatments include inorganics such as silicofluorides, alkali silicates, and alkaline earth hydroxides as well as synthetic organic polymer systems, e.g., acrylic polymers and copolymers, vinyl polymers, epoxies, waxes and

oils.[6] Organic consolidants satisfy some of the requirements for an effective protection system (good adhesion, increased mechanical strength) but fail to provide long-term stability upon exposure to ultraviolet light. Alkoxysilanes, e.g., tetraethoxysilane (TEOS) and methyltrialkoxysilanes (MTEOS and MTMOS), have been considered for use as stone consolidants because of their high penetrating ability and excellent UV stability. MTMOS consolidants were investigated, and briefly commercialized as *Brethane*, in the 1970s.[7,8] Although these simple alkoxysilane consolidants are stable to UV radiation and offer moderate protection to sandstones (silicates), generally they have not been effective on limestones and marble (carbonate rock). MTMOS based systems as well as commercial TEOS-based treatments[9,10] have shown little ability to adhere to and consolidate carbonate materials.[11] Conservators at The Getty Conservation Institute agree that "it is generally acknowledged that effective consolidants for limestone have not yet been identified."[12]

**Weathering of Stone.** Sandstones and limestones are extensively used throughout the world in art and architecture but are extremely susceptible to environmental deterioration. The most common *chemical* form of weathering is the hydrolytic attack of mineral surfaces. For siliceous rocks such as sandstone, this takes the form of a dissociative chemisorption process involving water adsorption followed by hydrolytic cleavage of the siloxane (Si-O-Si) bond. This process ultimately leads to the formation of an adherent, hydrated silica layer that is continually removed through further hydrolysis or mechanical erosion. Limestone undergoes a completely different form of chemical weathering. At moderate to low pH values[#], it is believed that three types of surface controlled reactions work in concert to solvate the calcium and carbonate ions:[14]

$$CaCO_3 + H^+ \underset{k_{-1}}{\overset{k_1}{\Longleftrightarrow}} Ca^{2+} + HCO_3^- \qquad (1)$$

$$CaCO_3 + H_2CO_3^* \underset{k_{-2}}{\overset{k_2}{\Longleftrightarrow}} 2\,HCO_3^- + Ca^{2+} \qquad (2)$$

$$CaCO_3 + H_2O \underset{k_{-3}}{\overset{k_3}{\Longleftrightarrow}} Ca^{2+} + CO_3^{2-} + OH^- \qquad (3)$$

[#] Rain water in equilibrium with atmospheric $CO_2$ at STP has a pH of 5.6. The effect of acidic atmospheric contaminants may lower the pH considerably and accelerate weathering. In the eastern U.S., the pH of most rainfall varies from 3.9 - 4.5.[13]

Under the conditions expected for monument weathering, reactions (1) and (2) dominate the surface chemistry. $H^+$ and dissolved $CO_2$ (as $H_2CO_3^*$, carbonic acid formed as atmospheric $CO_2$ dissolves in rainwater) are the key reactants in (1) and (2), respectively. In (2), the concentration of dissolved $CO_2$ is controlled by an equilibrium reaction with the gas phase. As the dissolved species are rapidly removed, fresh calcite surface is continually exposed. The net reaction can be summarized as:

Dissolution: $R_f = k_1 a_{H^+} + k_2 a_{H_2CO_3} + k_3 a_{H_2O}$

Precipitation: $R_b = k_{-1} a_{Ca^{2+}} a_{HCO_3} + k_{-2} a_{Ca^{2+}} a^2_{HCO_3^-} + k_{-3} a_{Ca^{2+}} a_{CO_3^{2-}}$

$$\text{Net Rate, } R = R_f - R_b$$

*Physical* weathering is largely a consequence of the adsorption of water in the native porosity of the rock. Freezing and thawing of ice within the pores, along with salt crystallization that results from continual wetting and drying causes spalling, scaling, flaking, and granular disintegration. Whereas chemical weathering removes material atom-by-atom, physical processes can remove cubic centimeters of material and, thus, represents a more serious threat to all rock types. A recent study estimated recession of ~15 μm per year from rain-washed marble surfaces exposed in the south central U.S.[15] Exposure to ambient concentrations of $CO_2$, rather than $SO_2$ or $NO_2$, was found to dominate marble solubility.

In summary, limestones are much more reactive than sandstones toward hydrolytic corrosion. Commercial conservation treatments have proven reasonably effective for sandstone, but due to the ionic nature of the surface and the hydrolytic lability of Ca-O-Si bonds formed using commercial (i.e., non-mineral-specific) products, there currently exist no effective, long-term treatments for limestones. Clearly, a mineral-specific approach based on understanding the interaction of candidate surface treatments with the calcite surface is needed to solve this problem.

**Requirements for protection of calcite minerals.** An ideal stone preservation scheme must address both chemical and physical modes of deterioration.[6] Effective treatments must (1) passivate the weathered mineral surface against further attack, (2) impart hydrophobicity to the rock to prevent water adsorption and the associated problems of freezing and thawing and salt crystallization, and (3) strengthen or consolidate the

surface to arrest further degradation. The treatment must be easy to apply, remain UV stable, and preserve the natural appearance of the stone. Additionally, the material must provide adequate depth of penetration into the interior of the stone and adhere to the mineral surface. For example, surface passivating agents should penetrate deeply into the termini of fissures and pores, whereas, mechanical strengthening must occur primarily within the near-surface region to forestall granular disintegration. Treatment processes are further complicated by inherent heterogeneity within stone, i.e., differences in mineralogy, porosity, and object size/geometry. Complete surface sealing may be undesirable – residual water in pores within the stone may be trapped in subsurface regions where it is subject to freeze/thaw cycles or can contribute to interfacial delamination of the surface treatment. Such a treatment, i.e., one that is permeable to water vapor but which impedes liquid water flow, may permit salt deposition to occur upon water evaporation.

**Sandia Strategy for Limestone Protection.** To satisfy these diverse demands, we chose hybrid organic-inorganic sol-gel methodologies to develop mineral-specific treatments. We have designed a flexible, multifunctional passivation scheme, depicted schematically in Figure 1.

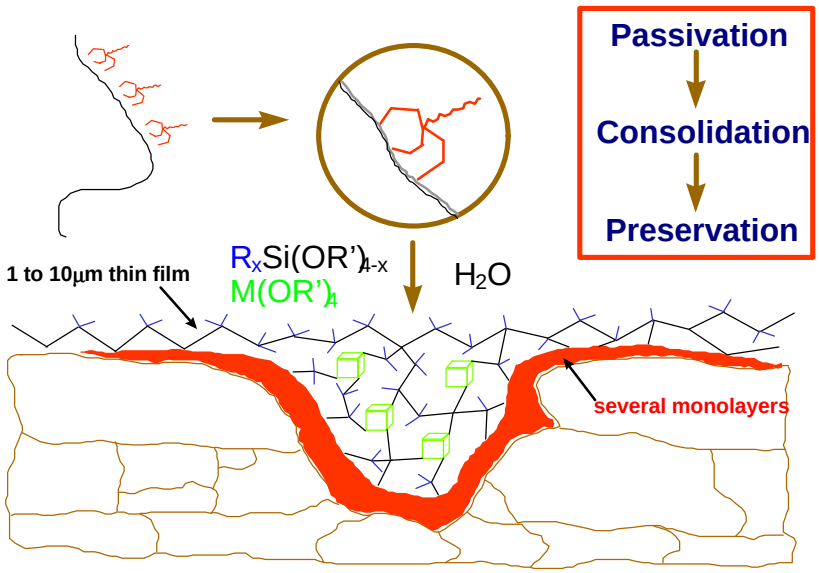


**Figure 1** Schematic diagram of a crevice in a limestone sculpture, coated with a passivant (shaded layer) plus alkoxysilane consolidant (1 to 10 μm outer thin film). The sketch in the upper left shows a tridentate passivant (e.g., SAAC) attached to the surface of the sculpted "nose." Optionally, Si or Zr oxides (*e.g.*, $M(OR')_4$) can be added to the alkoxysilane layer to increase mechanical strength and limit shrinkage.

Our protection strategy utilizes a bifunctional passivation layer that serves to selectively bind to the calcite surface while providing polymerizable sites for the reaction of a subsequent consolidation layer. While silylation with simple alkoxysilanes may be appropriate for sandstones, passivation of limestones requires chelation of calcium with multidentate ligands such as carboxylates (e.g., EDTA) or polyphosphates. Carboxylates are recognized for their ability to sequester $Ca^{2+}$ from carbonate sources while calcium phosphates form insoluble cements (e.g., hydroxyapatite) for dental composites and bone reconstruction. Our strategy for consolidation involves *in situ* polymerization of polysiloxanes or other polymetaloxanes within the porous, granular exterior surface of the weathered rock. Upon exposure to ambient humidity, hydrolysis and polymerization will create a three-dimensional network covalently bonded to the tailored surface passivation agent. Optionally, dense oxide nanoparticles (e.g., Zr, Si) may be embedded into the polysilicate matrix to create a filled composite structure and, thus, further improve mechanical integrity. The dispersion of molecular weights allow control of the depth of penetration of the different solution components. The organic R' ligands impart hydrophobicity to the consolidant and control wetting during application. UV stable R' ligands such as methyl, ethyl, phenyl and their fluorinated counterparts, e.g. $F_3C(CF_2)_n$-, are preferred to enhance the long-term outdoor stability of the treatment.

Representative structures of three classes of candidate passivants are depicted in Figure 2. In each case, the chelate moiety binds surface calcium ions while the sol-gel polymerizable "tail" presents reaction sites to a subsequent alkoxysilane-based consolidant. By varying the nature of the R and R' groups, the passivant "tail" can be modified to tailor (1) its relative affinity for the consolidant vs. the surface, (2) the rate of reaction by hydrolysis and condensation, and (3) the extent of water permeability in the passivation layer. The passivant thus is designed as an **interfacial coupling agent** between the carbonate surface and the sol-gel derived consolidant. The three candidate passivant molecules were selected based on their potential bonding configurations with surfaces of calcite ($CaCO_3$): **Class I --** silylaminocarboxylates (SAAC; e.g., Si-EDTA) with three carboxylate ligands that will exhibit a high affinity for $Ca^{2+}$; **Class II --** silylphosphonates (SAP) with strong P-O bonds which mimic hydroxyapatite mineralization; and **Class III --** aminoalkoxysilanes, e.g., aminoethylaminopropylsilane (AEAPS).

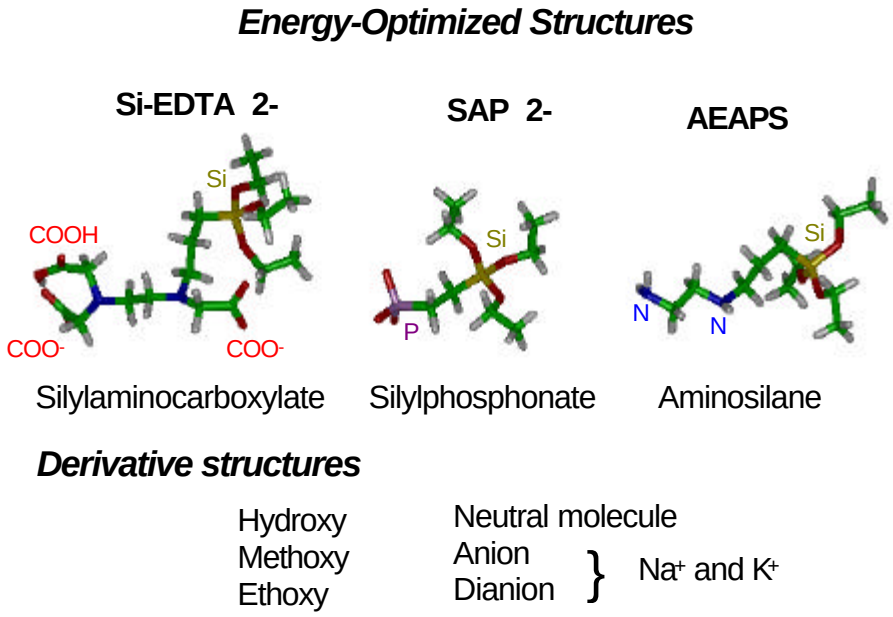


**Figure 2** The three candidate passivant classes and a listing of their derivatives with respect to the silane tail (left) and form of the passivant molecule that reacts with the surface (right).

The ability of this treatment strategy to retard calcite dissolution under simple simulated weathering conditions was tested by applying candidate passivants to calcite powders and cores in single or multiple coatings with and without a coating of alkoxysilane consolidant. Our goals were (1) to test the usefulness of molecular modeling for predicting effective passivants against their actual performance in aqueous environments, and (2) to demonstrate that a combined passivant/consolidant material is capable of protecting carbonate-based rocks from weathering.

## Methods and Procedures

**Computational Models.** Molecular modeling was used to evaluate the suitability of candidate passivants and several derivative structures for binding to calcite mineral surfaces. The total energy of the chemical system was monitored as a function of the atomic positions based on the energy contributions of bond stretching, bending, and torsion of the passivant molecule and the nonbonded interactions (Coulombic, short-range repulsive, and van der Waals). Energy-minimized configurations were first obtained for the isolated passivant molecule (see Figure 2), and then allowed to re-equilibrate under the influence of a calcite surface. The common (104) and (100) cleavage surfaces of calcite were created as periodic 29 Å x 29 Å lattices with a surface spacing of 25 Å. All atoms were constrained to their observed

structural positions with the calcium ion maintained at its full ionic charge (2+) and the carbonate charge (2-) partitioned among carbon (0.919) and oxygen (-0.973). Since the passivant solutions are typically applied to the stone at fairly high pHs, the exposed calcite surface is expected to be dominated by $Ca^{2+}$ and $CO_3^{2-}$.[16]

Monte Carlo simulations of the sequential packing of individual passivant molecules onto the calcite (104) surface were used to evaluate the expected surface coverage of the molecules. The simulations rely on a random sampling of a 29 Å x 29 Å x 25 Å volume such that a packing configuration is not accepted unless the energy falls below a critical value. Ten separate packing simulations using four passivant molecules each were performed, followed by energy minimization of the molecules.

**Preparation of passivant solutions.** Class I passivants were prepared from the reaction of silylpropylamine derivatives with chloroacetic acid and potassium hydroxide in methanol. Dilution to ≤ 5% (w/w) in methanol yielded passivant solutions that were stable for at least one year at room temperature. Concentrations greater than 10% frequently resulted in slow crystallization of the product on container walls. Solids prepared by rotary vacuum evaporation of solvent were highly condensed, but remained soluble in warm methanol. Products were confirmed by solution and solid state NMR ($^{29}Si$ and $^{13}C$) spectroscopy and FTIR spectroscopy. Condensation between silyl groups prevented the unambiguous assignment of SiOH vs. SiOR peaks. Reduced condensation may be achieved by replacement of KOH by $CaOCH_3$ or triethylamine; either base will eliminate water as a by-product of passivant synthesis.

Class II passivants were prepared from the reaction of trimethylphosphite and chloropropyltriethoxysilane under argon atmosphere with evolution of chloromethane as a by-product. Calcite powders were coated with dilute solutions of either the in-house preparation or a commercially available SAP-triethoxy preparation. Unlike the commercial Class I Si-EDTA-trisilanols, the commercial Class II passivant is nonaqueous and monomeric as sold. As neutral species, derivatives in Class II avoid contamination by salts and appear to offer better control over self-condensation.

Aminoethylaminopropylsilane (AEAPS) was used as a representative Class III passivant. AEAPS is commercially available (Aldrich Chemical Co.) and was used as a 3% or 25% (w/w) solution in methanol.

**Coatings on calcite: passivants and consolidants.** Candidate passivant solutions were prepared as described above and diluted in methanol as required. Calcite powder (Aldrich Chemical Co., low alkali $CaCO_3$) was pretreated to remove fines by adding an excess volume of methanol, ultrasonically agitating for 5 minutes, decanting the methanol, and air drying at 50°C. Ten grams of $CaCO_3$ powder was added to 40 ml of passivant solution while stirring. The solution was ultrasonically treated for 2 minutes to promote complete wetting of the powder and to minimize agglomeration. The passivant/powder solution was stirred at room temperature for at least 30 minutes and filtered through a 1 micron Teflon filter. The damp filter cake was gently broken up and allowed to dry at 50°C. For multiple coatings, the dried powder was resuspended in the passivant solution and the process repeated. During application of multiple coatings at high passivant concentrations (i.e., 25 wt%), filtration through a 10 micron filter was necessary.

A sol-gel derived consolidant was chosen from a family of silica sols prepared using a one- or two-step acid catalysis procedure.[17] These sols, formulated to promote maximum condensation, were developed for gas separation applications and yield films with tailored microporosity. Two consolidants were chosen for these preliminary tests: (1) a partially hydrolyzed TEOS solution with 50% w/w silica designated as "A2** stock" solution, and (2) a more highly polymerized, dilute sol containing 15% w/w silica designated "A2** 1:2".

After separating the passivated powder from the passivant solution, the damp powder was resuspended in consolidant solution to encourage polymerization between the reactive termini of the passivating molecule and the alkoxysilane consolidant. The suspension was treated ultrasonically for 2 minutes and stirred for 30-60 minutes at room temperature. Following filtration through a 1 micron Teflon filter, the powder was dried under ambient conditions to encourage further reaction with atmospheric moisture.

Coatings were deposited on limestone cores (nominally 75 mm long x 7.5 mm diameter) using vacuum impregnation (as described in a later section). Although this technique may prove impractical as a coating methodology for all but small artifacts, it was utilized to minimize sample-to-sample variation resulting from slight differences in core microstructure or variability in sol properties (viscosity, surface tension effects, and vapor pressure). Vacuum impregnation is in commercial use to facilitate deep penetration of epoxy resins into stone objects.[18]

**Calcite dissolution experiments.** Coated and uncoated calcite powders were tested under controlled conditions in "pH-stat" experiments[19] at 25°C (Figure 3). The leach test simulant solution was produced by constant bubbling of 20% $CO_2$ in $N_2$ through water to facilitate pH control at pH = 5, representing a mildly acidic rain. After adding 0.25 g of calcite (0.358 $m^2/g$) to the pre-equilibrated stirred solution, the pH was adjusted to 5 by the dissolution process and by base (0.1 N NaOH) addition. After the initial pH adjustment, pH was maintained to within ± 0.01 pH units by constant addition of 0.1 N HCl at a rate proportional to the rate of calcite dissolution. Total elapsed time of an experiment was at least 30 minutes.

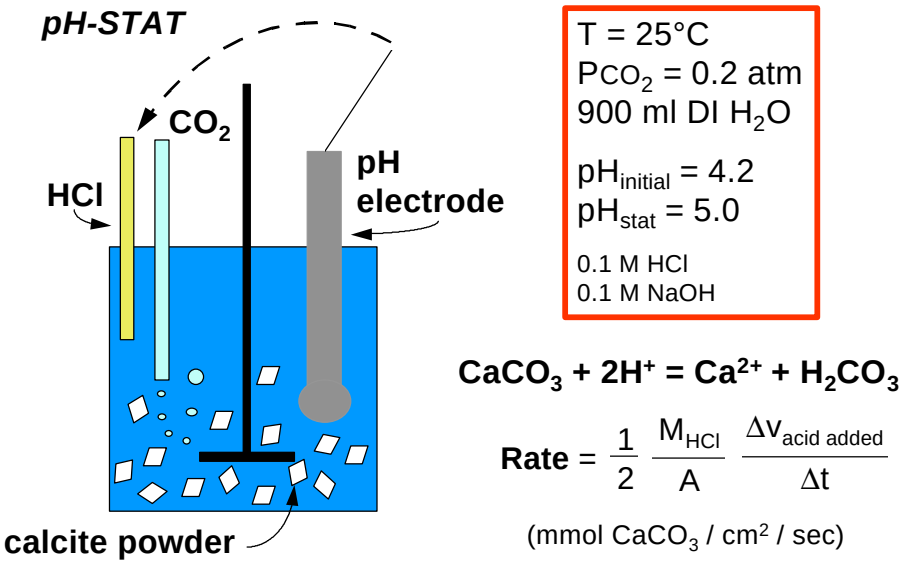


**Figure 3.** Schematic diagram of pH-stat apparatus and calculation of dissolution rate.

**Magnetic Resonance Imaging (MRI).** Magnetic resonance imaging was used to monitor water uptake in limestone cores (47 mm diameter x 177 mm long) as a function of time and consolidant. MRI experiments before and after treatments were performed on a Quest 4400 (Nalorac) spectrometer running on a VAX station II/GPX. Proton images were obtained at a resonance frequency of 80.33 MHZ using a 1.89T magnet with a 31 cm bore. A homebuilt probe utilizing a 2-turn solenoid coil (4.45 cm diameter x 12.7 cm long) was used. The two dimensional images were 128 x 128 points, resulting in a spatial resolution of approximately 1mm x 1mm x thickness of sample. The images obtained utilized a phase encoded spin echo pulse sequence, with only the Y and Z gradients employed.

**Nuclear Magnetic Resonance Spectroscopy (NMR).** The $^{29}Si$ NMR spectra were recorded at 39.6 MHz on a Chemagnetics console interfaced to a General Electric 1280 data station. The methanol solutions were 2.2 M MTMOS and 16 mM chromium acetylacetonate, a spin relaxation agent. $^{1}H$ broad-band decoupling was applied only during data acquisition in order to suppress any residual negative nuclear Overhauser effect. The $^{29}Si$ spin-lattice relaxation time of the monomer was approximately 4 seconds and a pulse repetition time of 15 seconds was employed.

**Scanning Probe Microscopy (SPM).** Scanning Probe Microscopy (SPM) was used to monitor the surface changes on single crystal calcite,[20] the primary mineral in limestone and marble. SPM is a technique by which an atomically sharp probe is raster-scanned across the surface being examined. The surface features are detected by deflections of a laser beam bounced off the probe. Each sample was observed at high resolution during four stages of the experiment: (1) prior to application of surface treatment, (2) during treatment, (3) after the application of protective treatments, and finally (4) while undergoing simulated weathering (exposure to acid rain simulant solution). A fluid cell microscope attachment (Nanoscope III, Digital Instruments, Santa Barbara, CA) was used to facilitate the injection of solutions.

Optically clear calcite samples from Chihuahua, Mexico were cleaved to expose the (104) surface. These samples were used to allow direct observation of dissolution of calcite when exposed to corrosive solutions; dissolution is characterized by etch pit formation and step retreat on the surface. Samples were placed in the passivant solution for 30 minutes, rinsed with methanol (solvent for the passivant solutions) and placed in the consolidant for an additional 30 minutes. Upon removal from the consolidant, the samples were rinsed in ethanol (solvent for the consolidant solutions) and dried in an oven at 60°C. A 12 µm SPM piezoelectric scanner (Model-E) and $Si_3N_4$ probes were used. The scan size was held constant between 4-10 $\mu m^2$, the Z-range was < 25 nm, and the scanning rate was 4-8 Hz which resulted in an image-acquisition time of less than 90 seconds. To simulate acid rain weathering, freshly deionized water (18 MΩ•cm) was allowed to equilibrate with atmospheric $CO_2$ for approximately 15 minutes and filtered through a 0.2 µm nylon membrane filter (Acrodisc-13, Gelman Corp.) prior to use. The pH of the deionized water was approximately 5.5.

**Environmental Scanning Electron Microscopy (ESEM).** The environmental SEM used in these experiments (ESEM Model E-3, Electroscan Corp., Wilmington, MA) facilitates the observation of materials in their natural and/or wet state without coating and drying. A microinjection system allows

for the introduction of liquids onto the samples while they are examined at high magnification. Concentrated sulfuric acid (pH~0) was used to simulate aggressive attack on the limestone. The microscope was operated at an accelerating voltage of 10-25 keV with a lanthanum hexaboride ($LaB_6$) electron emitter. Water vapor was used as the standard imaging gas. Untreated calcite samples were observed first at high magnification to establish baseline images. Finally, acid was introduced onto the samples using the microinjection syringe and the samples were re-imaged.

**Strength Tests.** Monks Park limestone cylinders (7.5 mm diameter x 75 mm long) were cut perpendicular to the bedding plane from stone quarried at Bath, England. The surface area of these limestone cores was 2-3 $m^2/g$ as determined by nitrogen gas adsorption. Analysis by mercury intrusion porosimetry yielded a porosity of 24%. Eight cores per treatment were dried at 60°C overnight before being treated with passivant and/or consolidant solutions. Each untreated core was evacuated in a Schlenk tube (valved glass tube) to a pressure of ~80 kPa. Passivant solution was then injected into the tube until the core was completely submerged and held for 2 hours. The passivant solution was removed and the consolidant solution was added to the damp core. The core was exposed to the consolidant for 2 hours to encourage *in situ* polymerization between the passivant-coated core and the consolidant. Unreacted consolidant was decanted and the cores were allowed to cure under ambient temperature/humidity conditions for 12 hours to allow further condensation by atmospheric moisture. Final drying occurred at 60 °C over a 24 hour period. The modulus of rupture of untreated and treated cores was determined from 3-point bend tests that approximated the ASTM method C674-88.[21] The ASTM test used a one KN load cell and a crosshead speed (loading rate) of 0.2 mm/minute.

## Results and Discussion

**Computer Simulations/Modeling.** Periodic boundary conditions (PBC) were used to model the optimum docking configuration of each candidate passivant on the calcite surface (see Figure 4). Two common calcite surfaces were examined in this fashion; the dominant rhombohedra (104) cleavage surface and the hexagonal prism (100) surface. Relative binding energies are obtained by calculating the subtracting the gas-phase energy of the passivant molecule and the energy of the isolated surface from optimized molecule-surface energy. The figure provides the optimized position of the Class I triethoxy-SAAC passivant on the (104) surface. The silane tail is appropriately positioned upward for future attachment and polymerization with the siloxane consolidant. The general trend of the passivant binding

energies is: SAAC > SAP > TEOS > AEAPS. Additionally, we observed the general trends: dianion > monoanion > neutral; trimethoxy > triethoxy > trihydroxy. Similar trends were observed for the (100) surface, but the binding energies were smaller.

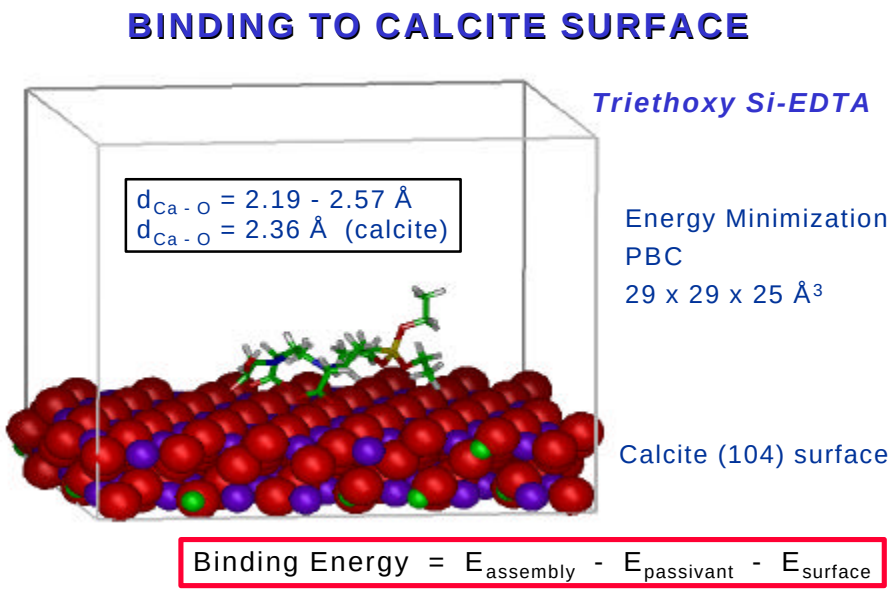


**Figure 4.** Molecular model showing the binding configuration of triethoxy Si-EDTA (SAAC) molecule to common cleavage surface of calcite ($CaCO_3$).

Figure 5 provides the plane view of the triethoxy-Si-EDTA (SAAC) passivant on the (104) surface as energy-optimized. The surface calcium atoms are highlighted to indicate the positioning of the carboxylate ligands among the $Ca^{2+}$ ions. Due to the periodic nature of the surface, the controlling electrostatics positions the three coordinating ligands between $Ca^{2+}$ pairs. Intramolecular steric effects within the SAAC molecule prevent an idealized positioning, however, the three carboxylate groups (one neutral and two deprotonated) provide a considerable amount of binding of the passivant to the surface. The experimental evidence suggests that the dianion SAAC compound binds so strongly to the calcite surface that some dissolution of the calcite occurs.

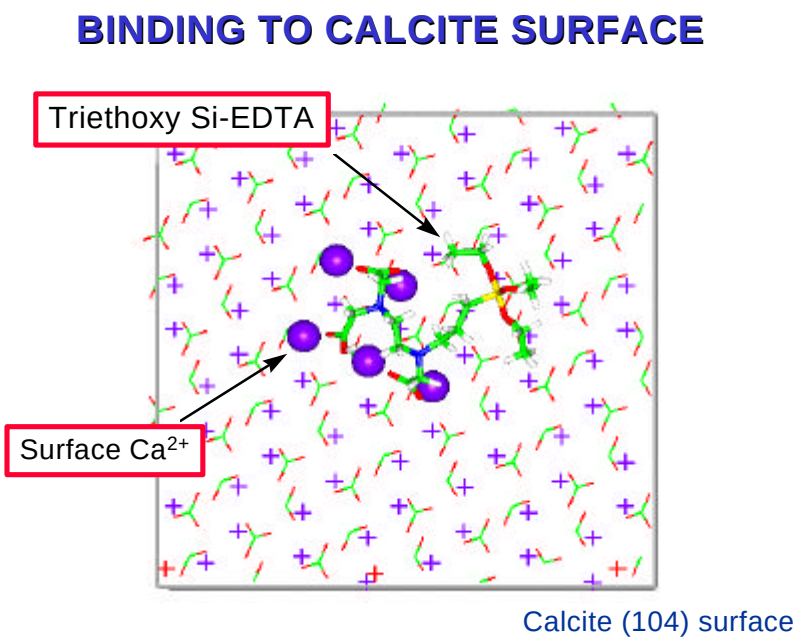


**Figure 5.** Plane view simulation of Class I triethoxy-Si-EDTA to calcite (104). Surface $Ca^{2+}$ atoms are highlighted to show positioning of carboxylate ligands.

A Monte Carlo packing simulation was performed for each of the candidate passivants on the (104) calcite surface, as shown in Figure 6 for triethoxy-Si-EDTA. These calculations suggest the optimum packing and surface concentration that would occur as the surfaces are coated and saturated during passivant treatment. Optimum solution concentrations could be obtained to ensure an efficient monolayer coverage. A sampling volume covering approximately 900 $Å^2$ of the calcite surface was defined and then used to sequentially introduce four passivant molecules. Approximately 50,000 configurations were examined with a critical energy required before acceptance of the ten optimum configurations. The lowest energy configuration was then used to determine bonding geometries and packing densities. Approximately 175 to 200 $Å^2$ per passivating molecule were observed for the triethoxy derivatives for the three candidate molecules. The greatest coverage was observed for SAP and the least by AEAPS.

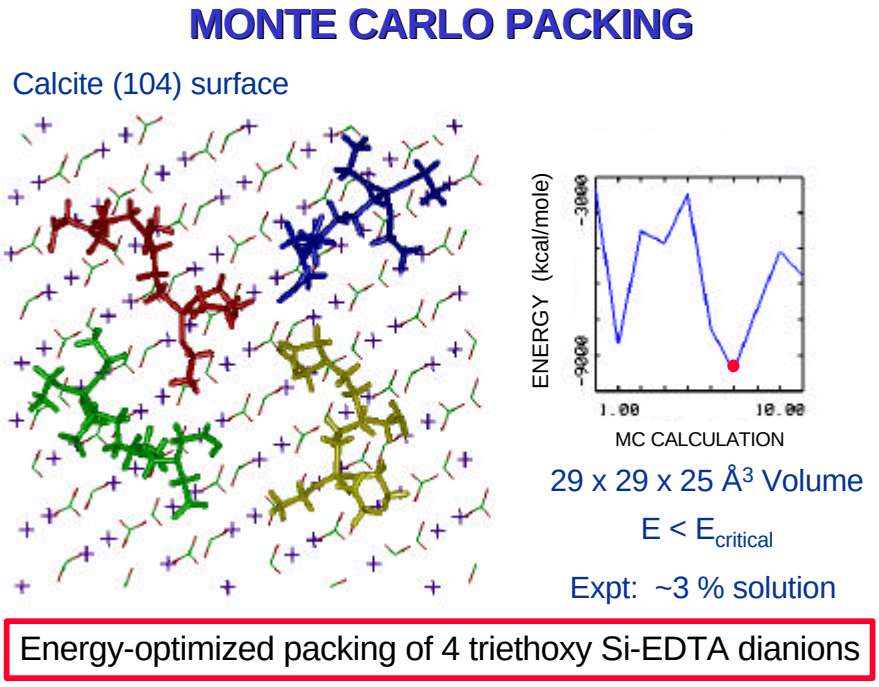


**Figure 6** Monte Carlo packing simulation for multiple Class I molecules.

Other molecular modeling calculations included the examination of water solvation (up to 100 molecules) about the energy-optimized configuration for each passivant on the calcite surface. The results of energy minimization and molecular dynamics simulations for this process suggest that the passivant binding remains unperturbed and the water molecules simply solvate the passivant. Gas phase calculations of each passivant molecule with an isolated $Ca^{2+}$ were performed to evaluate the ability of the passivants to bind and remove cations. Absolute binding energies are obtained and range from 110 kcal/mole for AEAPS, to 490 kcal/mole for the SAAC, and to 622 kcal/mole for the SAP passivant (all triethoxy derivatives). The greater binding strength of the SAAC and SAP molecules is related to their charged character. The modeling results suggest that the AEAPS would not necessarily lead to any substantial increase of calcite dissolution. The experimental leach tests of the various treated calcite powders support these modeling conclusions.

**MRI Results.** Proton images for three untreated core samples (designated B1, B2, B3) from the same limestone bed orientation were obtained as a function of contact time with water to monitor water penetration through the core. The core samples were pre-dried in an oven at 90°C for 5 days, and then the edges were treated with epoxy. The bottom (non-epoxied) surface of

the core was contacted with water and weighed and imaged after 5, 10, 15, 45 and 105 minutes. At 105 minutes, the proton images showed that the cores were still not fully saturated. Weight vs. time curves for these samples showed variability between samples sufficient to warrant baseline imaging of each sample prior to coating. Differences in porosity, mineral composition (e.g., due to the presence of quartz veins), or paramagnetic impurities likely account for observed deviations in water uptake. Baseline time-resolved water uptake experiments on untreated stone cores demonstrate the utility of MRI analysis for the evaluation of protective treatments on monolithic samples. Orientation of exposed surfaces in relation to their orientation in the original quarry bed noticeably affects water uptake rates. Two dimensional projections of water density in the cores as a function of contact time with water have a resolution of approximately 1 mm. Most samples show sharp water penetration boundaries. Untreated cores adsorbed approximately 13 kg/m$^2$ of water.

Two of the cores were treated using surface applications of commercial consolidants. Sample B1 was coated with 2 coats of Conservare® OH (total coating weight of 0.2 g). Sample B2 received 2 coats of Conservare® H (total coating weight of 0.5 g). The coated samples were allowed to air dry for 1 week prior to imaging studies. Imaging results (not shown) suggest only minimal water adsorption following the 105 min exposure: 0.07 kg/m$^2$ for B1, 0.16 kg/m$^2$ for B2, compared to 13 kg/m$^2$ for the untreated control core (B3). These results formed the basis for subsequent evaluations of passivant and consolidant treatments.

**NMR Results.** While alkyl alkoxysilanes are widely used for the conservation of murals and paintings, the effect of foreign materials on the kinetics and mechanisms of the sol-gel process is not well-understood. Methyltrimethoxysilane (MTMOS) is a simple organosilicon monomer that can be used to represent more complex structures in initial studies.

The uncatalyzed hydrolysis and polycondensation reactions of MTMOS were monitored by $^{29}$Si NMR as a function of reaction time, both with and without calcite powder present, throughout the reaction period. The sample reacted for 24 hours shows signals characteristic of $T^0$, $T^1$, $T^2$ and $T^3$. The T distributions and extents of reaction as a function of time are listed in the following table.

**Table I. $^{29}$Si NMR data of MTMOS-Methanol-water mixture ± Calcite**

| MTMOS-Methanol-water mixture | | | | |
|---|---|---|---|---|
| | T Distribution | | | Extent |
| Time (h) | $T^1$ | $T^2$ | $T^3$ | of reaction |
| 0.5 | 29.9 | 2.4 | -- | 11.6 |
| 5.0 | 63.3 | 13.9 | -- | 30.3 |
| 24 | 64.4 | 23.4 | 1.8 | 38.9 |
| **MTMOS-Methanol-water mixture reacted with calcite** | | | | |
| 0.5 | 2.4 | -- | -- | 0.8 |
| 5.0 | 2.7 | 2.4 | -- | 2.5 |
| 24 | 27.0 | 9.6 | 2.6 | 18.0 |

The extents of reaction, defined as the percentage of Si-O bonds that bridge neighboring Si sites, were much lower for samples that contacted calcite. Clearly, calcite significantly retards the condensation of MTMOS. This conclusion quantitatively agrees with studies in other laboratories which conclude that calcite retards the condensation reactions of simple alkoxysilanes into a consolidating network.[22,23]

**Leaching Studies.** Dissolution rates from 24 experiments with three candidate passivants are summarized in Figure 7 and compared with a common commercial product. A complete tabulation of the dissolution rates for all 24 experiments is included in Appendix A.

A number of observations can be made. First, the order of effectiveness is reversed from that predicted using the relative binding energies determined by molecular modeling. Second, neither single nor multiple coatings of the passivants alone significantly reduce the rate of calcite dissolution. Third, all passivants when linked to a single coating of the sol consolidant result in slower dissolution rates. The most significant decrease occurs with the AEAPS passivant. Fourth, the effectiveness of the passivant in binding to the consolidant is higher when the passivant is applied from a higher concentration solution. Fifth, the AEAPS passivant plus consolidant (50% TEOS) combination is more effective than the commercial product Conservare® OH (~ 75% TEOS from Wacher Chemie), and at least as, if not slightly more, effective than Conservare® H which includes a hydrophobic agent. We note that neither of the Wacher commercial products are recommended for treatment of carbonate stone. In comparing these results, we devised a coating procedure for powders, and

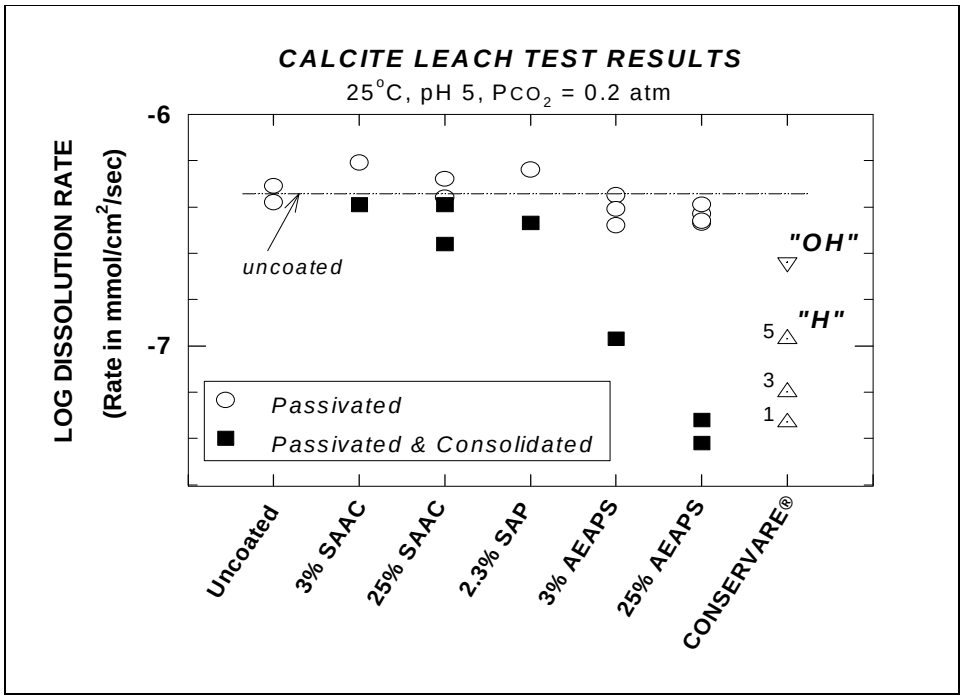


**Figure 7.** Dissolution rates of uncoated and coated calcite powders. All samples coated with passivants + consolidants yield slower dissolution rates than uncoated calcite. Numbers next to Conservare® data points represent number of applied coatings.

as such, could not follow exactly the recommended procedures for application of Conservare® OH and Conservare® H. However, our procedures were used consistently for all materials. Sixth, multiple coatings of consolidant, as exemplified by the Conservare® H-coated samples, appear to show reduced effectiveness against dissolution.

The trend in dissolution rates contradicts the trend of the model predictions for passivant binding strength. This suggests a threshold binding energy above which the passivant enhances the dissolution rate. Interestingly, the calculated binding energy for TEOS, the primary component of our sol-gel consolidant and both commercial consolidants, lies between that of SAP and AEAPS. Similarly, the measured dissolution rate for calcite powder coated with Conservare® OH also lies between the rates for powders coated with SAP + consolidant and AEAPS + consolidant. The consolidant appears to play a role in inhibiting dissolution because all of the combination coatings acted to reduce dissolution rate. Although the binding energy of AEAPS is less than those of SAAC and SAP, AEAPS binds strongly enough to yield a new material that reduces the dissolution rate significantly. An added advantage of the AEAPS passivant is that it is commercially available and relatively inexpensive.

**Scanning Probe Microscopy.** Dissolution of untreated calcite was observed immediately upon addition of deionized water by the formation of etch pits approximately 200 nm along the diagonal and about 100 nm along the shorter diagonal (Figure 8a, b). The depth of the etch pits was about 0.5 nm which suggests that dissolution occurs in monomolecular steps. The rate of surface loss was 4-7 $nm^2$/sec. Further dissolution resulted in the retreat of steps and merging of adjoining pits (Figure 8b). This dissolution of calcite in the presence of an acidic undersaturated solution continues until equilibrium is reached in the fluid cell volume of the microscope. The surface etching immediately resumes when the cell is purged a second time with the leaching solution. This simple reaction allows a comparison of the relative passivation of the surface.

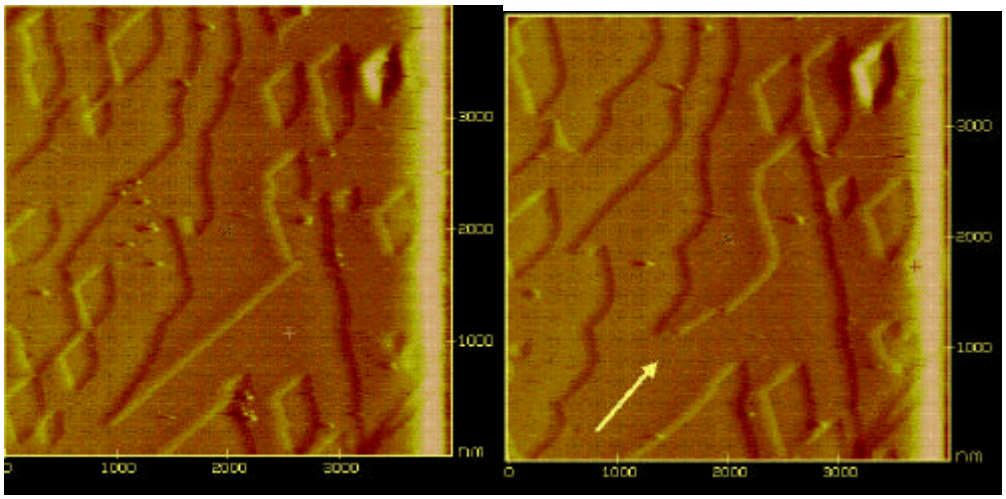


**Figure 8a, b.** SPM image (left) of single crystal calcite upon addition of simulated acid rain. The appearance of etch pits confirms rapid dissolution of calcite. The etch pits are diamond shaped (<1 nm deep). Figure 8b shows the same location after 3 additional minutes of exposure to the weathering solution. Note the enlargement of the etch pits and retreat of steps (especially the peninsular region in the center of the images).

Calcite crystals treated with the 3% SAAC passivant and A2** 1:2 consolidant (15% w/w) show no etch pit formation or step retreat upon addition of the weathering solution (Figure 9a, b). The steps are no longer visible and the surface appears rough. A triangular pattern of coating defects, visible as bright circles with dark inclusions, can be identified in both images. The increased contrast in Figure 9b is due to a deliberate

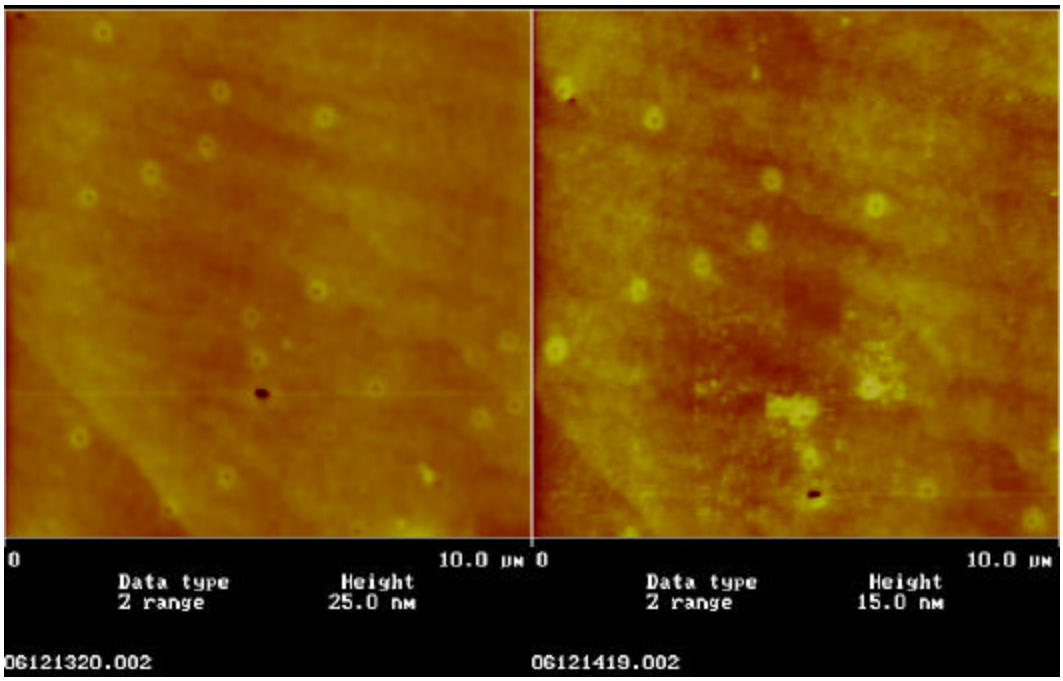


**Figure 9a, b.** SPM images of single crystal calcite treated with the SAAC passivant and A2** consolidant, before (left) and after (right) addition of simulated acid rain. Time elapsed between the two images is one hour. With the exception of increased contrast due to a change in the Z-axis scale, the surface remains unchanged. No etch pit formation or step retreat is seen.

decrease in the z-axis scale from 25 nm to 15 nm to highlight surface features. However, the calcite treated with the 15% silica consolidant alone also showed no etch pits or step movement and the contrast between these two samples can be enhanced, for example, by using a more corrosive solution. Thus, the protection of the calcite may be due simply to the inorganic framework on the surface. Calcite treated similarly with a commercial consolidant, Conservare® OH (75 % silica, not recommended for limestones), resulted in a film that cracked and peeled away from the surface. Samples treated with the AEAPS passivant alone were also tested and although some minor etch pits were seen, no large scale dissolution was observed. Also, the surface reacted layer of coupling agent was not removed upon addition of the simulated acid rain. The samples treated with AEAPS plus "A2** stock" consolidant retained their surface coating even upon addition of the simulated acid rain as shown in Figure 10.

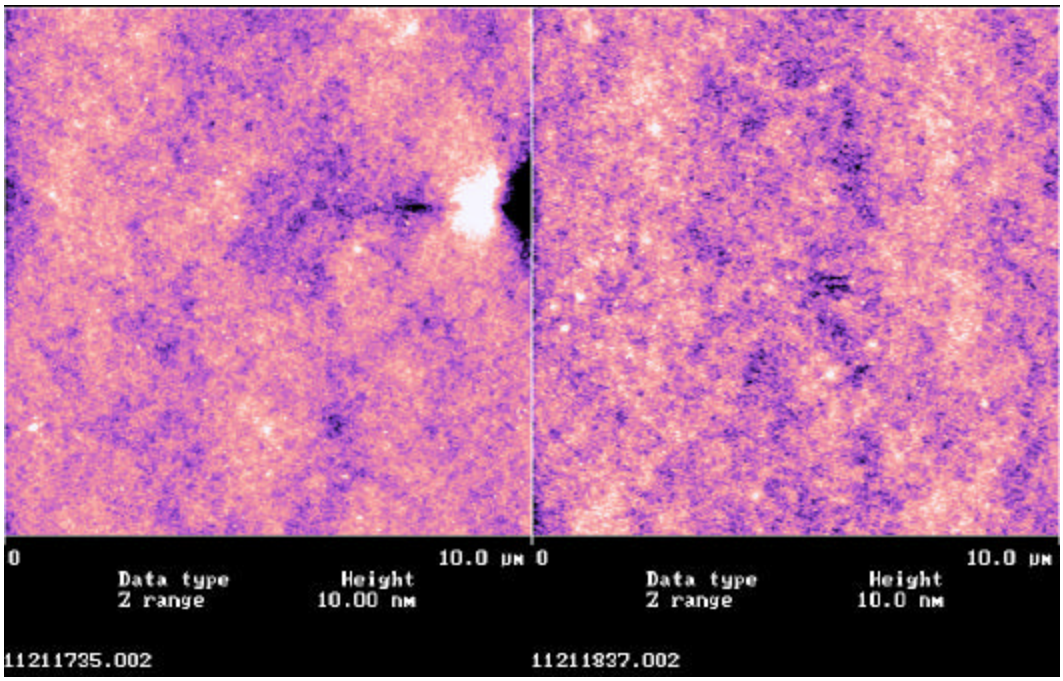


**Figure 10.** Calcite treated with 25% AEAPS plus A2**, before and after addition of DI water of pH ~5.5. Time elapsed between the two images is one hour. Note absence of etch pits. The high contrast region in the left image is a scanning artifact.

**Strength Tests.** The effect of the different protection treatments on the modulus of rupture of the limestone cores as determined from three-point bend tests is seen in Figure 11. The commercial consolidant, Conservare® H resulted in the greatest increase in flexural strength. Cores treated with A2** 15% silica consolidant alone (without a passivant), showed larger strength increases than stones treated with more concentrated A2** (50%).

This result is likely is due to differences in the nature of the polymer rather than simply the differences in concentration; the A2**15% sol is subjected to two acid-catalyzed hydrolysis steps (final $H_2O$:Si ratio ≈ 5), aging at 50°C to encourage complete polymerization, and dilution to an optimum concentration for film formation; whereas, the A2** 50% sol undergoes a simple single-step acid hydrolysis ($H_2O$:Si ratio ≈ 1) yielding a film with a tenuous, weakly branched structure.[17]

The increase in the concentration of the AEAPS passivant from 3% to 20% results in a 25% increase in strength and a 35% increase compared to the untreated stone. Other researchers have observed that incorporation of AEAPS into silica aerogels resulted in faster gelation rates and increases in bulk density (reductions in surface area).[24] The basic amino group in AEAPS

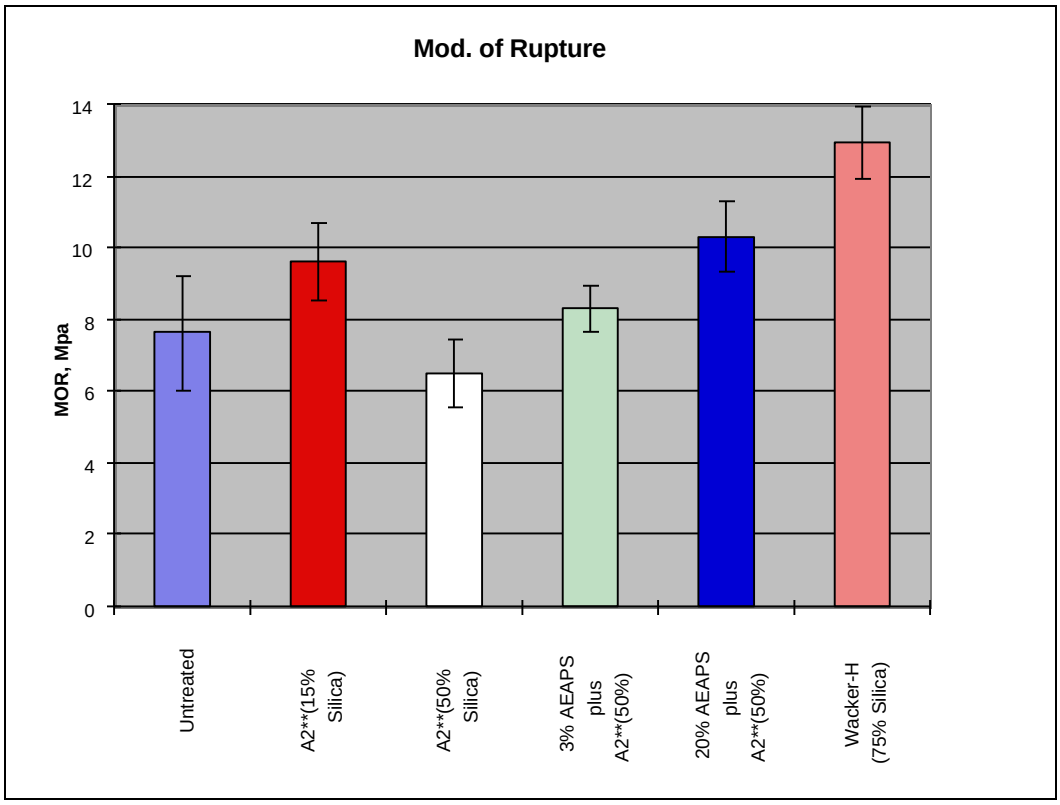


**Figure 11.** Plot of modulus of rupture for calcite cores with no surface treatment, consolidant alone, passivant + consolidant, and commercial sandstone consolidant. The measured standard deviations are large due to the inherent heterogeneous nature of the limestone cores.

may enhance the condensation reaction. Cores treated with the 20% AEAPS sol and 15% A2** sol were not tested due to rapid gelation on the surface. The gelation prevented effective penetration of the consolidant and led to the formation of excess gelled material on the surface of the stone. The trisilanol form of the SAAC passivant was eliminated in preliminary experiments. The SAAC passivant appeared to weaken the stone by binding too strongly to calcite and leaching $Ca^{2+}$ from the samples. The removal of $Ca^{2+}$ by the SAAC passivant was confirmed by analysis of the treatment solution before and after exposure to calcite. SAAC solutions used to coat limestone cores were evaluated for increased calcium ion concentration using Direct Coupled Plasma Spectroscopy and were found to have $Ca^{2+}$ concentrations five times higher than found in control solutions.

**Environmental Scanning Electron Microscopy (ESEM)** The untreated limestone is filled with *ooids* (concentric spherical structures) and consists of amorphous regions and polycrystalline phases of calcite (Figure 12a). Large voids amidst clusters of fine grained calcite in the limestone are seen. Figure 12b shows the same region after introduction of concentrated acid. Figure 13a shows limestone passivated with SAAC and consolidated with A2**; the composite coating has cracked and retracted exposing bare calcite. Upon exposure to acid, the bare areas exhibit corrosive attack whereas coated areas show no deterioration, suggesting that the protective treatment, if continuous, would retard acid-rain attack. The cracking may be the result of poor binding between the SAAC passivation layer and the calcite surface, allowing the biaxial tensile stress developed upon curing to cause cracking and delamination.[25] Improved coupling chemistry combined with a reduction in the coating thickness should remedy this behavior.

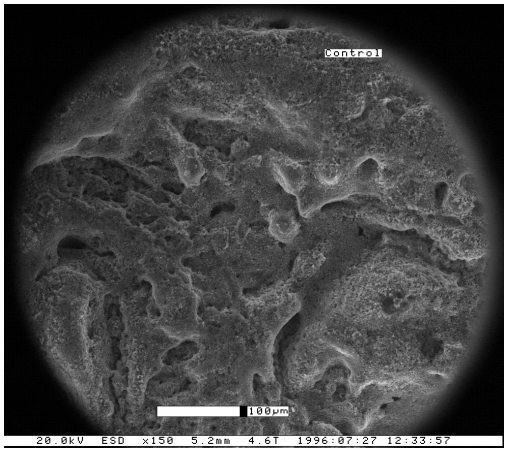


**Figure 12a, b.** Surface of untreated limestone shows *ooids* (concentric structures to the bottom left and right of Figure 12a) and polycrystalline regions (center). Figure 12b shows the same region after addition of acid. Micron bar =100 µm.

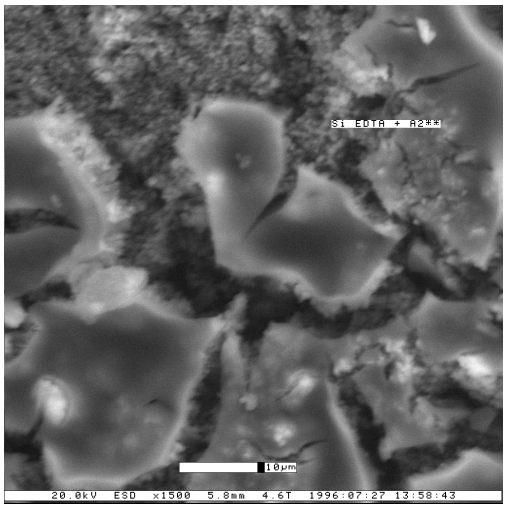


**Figure 13a, b.** Treated limestone before addition of concentrated sulfuric acid (Figure 13a). Inadequate coupling by the SAAC passivant led to shrinkage of the consolidant. Figure 13b shows the same region after addition of acid. The consolidated areas remain unaffected although the layer is cracked. Micron bar = 10 µm.

## Conclusions

Molecular models combined with dissolution experiments, microscopic imaging of untreated vs. treated surfaces, and strength tests constitute a rational approach for designing new materials for protection of carbonate-based structures and sculptures. Calculated relative binding energies and packing configurations can be used to develop a hierarchy of candidate passivant molecules and to explain dissolution rate data obtained in controlled pH-stat experiments. $^{29}$Si NMR results suggest that simple alkoxysilanes fail in carbonate conservation treatments because (1) they have low affinity for calcite, as demonstrated by modeling, and (2) calcite inhibits the condensation of simple alkoxysilanes into a consolidating network. Thus, passivation of the calcite surface is needed for effective use of alkoxysilane consolidants.

Computer simulations suggest a binding order (strongest to weakest) of SAAC>SAP>TEOS>AEAPS. Calcite dissolution rate experiments show that the actual order of effectiveness is reversed from that predicted; i.e., AEAPS treated samples showed low dissolution rates while SAAC treated samples had high rates. The contradictory trend in dissolution rates suggests a threshold binding energy above which the passivant actually enhances the dissolution of $Ca^{2+}$ from the surface. Although the binding

energy of AEAPS is less than those of SAAC and SAP, AEAPS binds strongly enough to reduce the dissolution of calcium when exposed to simulated acid rain conditions. During leach tests, all passivants exhibited even slower dissolution rates when linked to a consolidant layer. The AEAPS passivant in combination with a TEOS consolidant slowed the dissolution rate to 1/10 that of uncoated calcite. During simulated leaching studies, we identified one passivant/consolidant combination (AEAPS + A2** sol) that, *even in its unoptimized form*, performed substantially better than commercial Conservare® OH and at least as well as Conservare® H in short-term tests.

Environmental microscopy offers a means to subject limestone to *in-situ* corrosion tests. We determined, at a microscopic level, that calcite treated with AEAPS passivating coupling agent + A2** sol consolidant is resistant to corrosion by mildly acidic deionized water of pH 5.5. Three-point bend tests demonstrated that a 15% silica sol alone as well as a combination of 20% AEAPS + 50% silica sol strengthen limestone cylinders by as much as 25-35%.

Further experiments to optimize passivant concentration and functionality, consolidant chemistry and reactivity, as well as evaluation of commercial deposition (e.g. spray-coating) processes and characterization of long-term weathering durability are required to finalize this coating for commercial application. Novel functionalized treatments with cationic photoinitiators which polymerize the organic moieties using natural sunlight may yield further improvements in performance and greatly enhance processing. In addition to solving the urgent need to preserve our cultural treasures, the methodology described here can be applied to other mineral-specific corrosion problems such as the degradation of concrete infrastructure, environmental contamination by leached mine tailings, protection of ship hulls, and scale formation in petroleum wells.

## References


**1.** Amoroso, G. and V. Fassina, *Stone Decay and Conservation*. Materials Science Monographs **11**, Elsevier, Amsterdam (1983**)** 453.

**2.** Winkler, E. M. *Stone: Properties, Durability in Man's Environment.* 2nd Ed. Springer-Verlag, New York (1975).

**3.** Holloway, M. "The Preservation of Past", *Scientific American* (May 1995) 98.

**4.** Wheeler, G. S., A. Schein, G. Shearer, S. H. Su, and C. S. Blackwell, "Preserving Our Heritage in Stone", *Analyt. Chem*. **64/5** (1992a) 347-356.

**5.** Passaglia, E. In *Materials Degradation Caused by Acid Rain*, R. Baboian, ed., American Chemical Society Symposium Series **318**, Washington, D.C. (1986) 384-396.

**6.** Clifton, J. R., *Stone Consolidating Materials: A Status Report*, National Bureau of Standards Technical Note 1118, U.S. Government Printing Office, Washington, D.C. (May 1980).

**7.** Moncrieff, A., "The Treatment of Deteriorating Stone with Silicon Resins: Interim Report". *Studies in Conservation* **21/4** (November 1976) 179-191.

**8.** Arnold, L. and C. Price, "Alkoxysilanes for the Preservation of Stone", Building Research Station Note, HMSO (1976) 1-4.

**9.** Bosch, E., M. Roth, and K. Gogolak. US Patent 3,955,988 (1965).

**10.** Weber, H., "Stone Conservation – Planning and Execution", Conservare® Technical Bulletin 483-1, ProSoCo, Inc., Kansas City, KS (1985).

**11.** Wheeler, G. S., S. A. Fleming, and S. Ebersole, "Comparative Strengthening Effect of Several Consolidants on Wallace Sandstone and Indiana Limestone", in *Proceedings of the 7th International Congress on the Deterioration and Conservation of Stone* **1518**, Lisbon, Portugal (1992) 1033.

**12.** William S. Ginell, Head -- Architecture and Monuments, The Getty Conservation Institute, Marina del Rey, CA; personal communication (August 1995).

**13.** Baedecker, P. A., *et al*., "Effects of Acidic Deposition on Materials", NAPAP Report 19 *Acidic Deposition: State of Science and Technology*, National Acid Precipitation Assessment Program, U. S. Bureau of Mines, Washington, D.C. (1990).

**14.** Baedecker, P. A. and M. M. Reddy, "The Erosion of Carbonate Stone by Acid Rain", J. Chem. Educ. **70/2** (1993) 104-108.

**15.** Yerrapragada, S. S., S. R. Chirra, J. H. Jaynes, S. Li, J. K. Bandyopadhyay, and K. L. Gauri, "Weathering Rates of Marble in

Laboratory and Outdoor Conditions", J. Environ. Engr. (September 1996) 856-863.

**16.** van Cappellen, P., L. Charlet, W. Stumm, and P. Wersin, Geochim. Cosochim Acta **57** (1993) 3505.

**17.** Brinker, C. J., R. Sehgal, S. L. Hietala, R. Deshpande, D. M. Smith, D. Loy, and C. S. Ashley, "Sol-Gel Strategies for Controlled Porosity Inorganic Materials", J. Membrane Science **94** (1994) 85.

**18.** Ginell, W. S., P. Kotlik, C. M. Selwitz and G. S. Wheeler, "Recent Developments in the Use of Epoxy Resins for Stone Consolidation", Mater. Res. Soc. Symposium Proceedings **352** (1995) 823-829.

**19.** Plummer, L. N., T. M. L. Wigley, and D. L. Parkhurst, Amer. J. Sci. **278** (1978) 179.

**20.** Rao, S. M., C. S. Scotto, K. L. Nagy and C. J. Brinker, "Protection of Stone Against Weathering", *27th Technical Conference of the International Society for the Advancement of Materials and Process Engineering (SAMPE)*, Albuquerque, NM (October 1995).

**21.** "Standard Test Methods for Flexural Properties of Ceramic Whiteware Materials", ASTM Method C674-88, American Society for the Testing of Materials, Philadelphia, PA (1988).

**22.** Danehey, C., G. S. Wheeler and S. H. Su, *Proceedings of the 7th International Congress on Deterioration and Conservation of Stone*, **1518**, Lisbon, Portugal (1992) 1043.

**23.** Simon, S., B. Wrackmeyer and R. Snethlage (unpublished).

**24.** Husing, N., U. Schubert, B. Riegel, and W. Keifer, "Chemical Functionalization of Silica Aerogels", Mater. Res. Soc. Symposium Proceedings **435** (1996) 339-344.

**25.** Brinker, C. J. and G. W. Scherer, *Sol-Gel Science: The Chemistry and Physics of Sol-Gel Processing*, Academic Press, San Diego, CA (1990) 118, 124.

# Appendix A

## pH Stat Experiments of passivant/consolidants on calcite

| Expt. # | Passivant | # of Coats | Consolidant | # of Coats | Log Dissolution Rate |
|---|---|---|---|---|---|
| Ald6b | none | 0 | none | 0 | -6.38 |
| BlankCalcite | none | 0 | none | 0 | -6.31 |
| Ald4a | 3% SAAC | 1 | none | 0 | -6.21 |
| 112196-4 | 3% SAAC | 1 | A2** | 1 | -6.39 |
| 112296-1 | 25% SAAC | 1 | none | 0 | -6.36 |
| 112296-1r | 25% SAAC | 1 | none | 0 | -6.28 |
| 112296-2 | 25% SAAC | 1 | A2** | 1 | -6.56 |
| 112296-2r | 25% SAAC | 1 | A2** | 1 | -6.39 |
| 112296-3 | 2.3% SAP | 1 | none | 0 | -6.24 |
| 112296-4 | 2.3% SAP | 1 | A2** | 1 | -6.47 |
| 3%IIIb1c | 3% AEAPS | 1 | none | 0 | -6.35 |
| 110996-1 | 3% AEAPS | 5 | none | 0 | -6.41 |
| 110996-1r | 3% AEAPS | 5 | none | 0 | -6.48 |
| 112096-2 | 3% AEAPS | 5 | A2** | 1 | -6.97 |
| 110996-2 | 25% AEAPS | 1 | none | 0 | -6.43 |
| 111096-1 | 25% AEAPS | 5 | none | 0 | -6.47 |
| 111096-1r | 25% AEAPS | 5 | none | 0 | -6.46 |
| 111096-s | 25% AEAPS | 5 | none | 0 | -6.39 |
| 110996-3 | 25% AEAPS | 1 | A2** | 1 | -7.42 |
| 111096-2 | 25% AEAPS | 5 | A2** | 1 | -7.32 |
| 111796-1 | none | 0 | Conservare® H | 1 | -7.33 |
| 111996-1 | none | 0 | Conservare® H | 3 | -7.20 |
| 112096-1 | none | 0 | Conservare® H | 5 | -6.97 |
| Ald8 | none | 0 | Conservare® OH | 1 | -6.64 |

(rates are in units of mmol/cm$^2$/sec; ± 20% uncertainty)

# APPENDIX B

## Publications and Presentations


**1.** Cygan, R. T., C. S. Scotto and C. J. Brinker, "Molecular Modeling of Aminocarboxylate Passivants on Calcite Mineral Surfaces", *IV International Conference on Advanced Materials*, Cancun, Mexico (August 1995).

**2.** Rao, S. M., C. S. Scotto, C. J. Brinker, R. T. Cygan, K. L. Nagy, R. A. Assink and T. Alam, "Sol-Gel Preservation of Weathered Stone", *IV International Conference on Advanced Materials*, Cancun, Mexico, (August 1995).

**3.** Rao, S. M., C. S. Scotto, K. L. Nagy and C. J. Brinker, "Protection of Stone Against Weathering", *27th International SAMPE Technical Conference*, Albuquerque, NM, October 1995.

**4.** Rao, S. M., C. J. Brinker and T. J. Ross, "Environmental Microscopy in Stone Conservation", *Scanning* **18** (1996) 508-514.

**5.** Cygan, R. T., K. L. Nagy, C. S. Scotto and C. J. Brinker, "Weathering and Stabilization of Monument Materials" (Invited), Geological Society of America Abstracts with Programs **28** (October 1996) A359.

**6.** Nagy, K. L., R. T. Cygan, C. S. Scotto, C. J. Brinker and C. S. Ashley, "Use of Coupled Passivants and Consolidants on Calcite Mineral Surfaces", Mater. Res. Soc. Symposium Proceedings **462** (December 1997) 301-306.

**7.** S. M. Rao, C. S. Scotto, K. L. Nagy, R. T. Cygan, C. S. Ashley and C. J. Brinker, "Conservation of Monuments: A Surface-Specific Approach to the Design of Stone Preservatives", *5th Structural Studies, Repairs and Maintenance of Historical Buildings (STREMAH) Conference*, San Sebastian, Spain (June 1997).

**8.** S. M. Rao, C. J. Brinker and T. J. Ross, "Testing of Anti-Weathering Stone Treatments Using Environmental Scanning Electron Microscopy", *5th Structural Studies, Repairs and Maintenance of Historical Buildings (STREMAH) Conference*, San Sebastian, Spain (June 1997).

**9.** S. M. Rao, A. S. Sellinger, C. J. Brinker, C. S. Ashley, R. T. Cygan, K. L. Nagy, and C. S. Scotto, "Anti-Weathering Treatments for Mineral Surfaces", Materials Research Society's Spring Meeting, *Symposium O: Hybrid Materials*, San Francisco, CA (April 1998).

**10.** Rao, S. M., "Anti-Weathering Treatments to Protect Mineral Surfaces: Hybrid Sol-Gel and Biomimetic Strategies," Ph.D. Dissertation, University of New Mexico, Albuquerque, NM (anticipated April 1998).

# APPENDIX C

## Related Publications


**1.** Wu, Corinna, "Consolidating the Stone", *Science News* (cover story) **151/4**, Science Service, Washington, D. C. (January 25, 1997) 56-57.

**2.** "New Strides in Conservation?", *Art in America* **85/4**, Brandt Art Publications, Inc., New York (April 1997) 29.

**3.** "Pit Stop", *Discover the World of Science*, Disney Publications (July 1997).

**4.** Mgyatt, M., "Protective Coating: New Limestone Preservative Slows Wear and Tear on Landmarks", in *Chicago Tribune* **16/5F** (February 16, 1997) and "Scientists Develop a Coat of Armor for Monuments", in *Los Angeles Times* **A25** (March 9, 1997) Associated Press, New York, NY.

**5.** "Metropolitan Museum of Art and Sandia Work to Preserve National Treasures", *Sandia Lab News* **49/1**, Sandia National Laboratories, Albuquerque, NM (January 17, 1997) 1.

**6.** "Long-Life Limestone and Marble", *New Ideas*, Sheena Harold, Producer; Peter Goodwin, Presenter; British Broadcasting Co. (February 16, 1997).

**DISTRIBUTION:**

2 Dr. Kathy Nagy
University of Colorado
Department of Geological Sciences
2200 Colorado Avenue
Boulder, CO 80309

1 Dr. Cathy S. Scotto
Naval Research Laboratory
Optical Sciences Division
4555 Overlook Ave. SW
Washington, D.C. 20375-5338

4 Mr. Sudeep Rao
UNM/SNL Advanced Materials Lab
1001 University SE
Albuquerque, NM 87106

1 Dr. George Segan Wheeler
The Metropolitan Museum of Art
Sherman Fairchild Center for Objects Conservation
1000 Fifth Avenue
New York, NY 10028

1 Dr. William Ginell
The Getty Conservation Institute
4503 Glencoe Ave.
Marina del Rey, CA 90292-7913

1 Dr. Eric Doehne
The Getty Conservation Institute
4503 Glencoe Ave.
Marina del Rey, CA 90292-7913

| | | |
|---|---|---|
| 6 | MS 1349 | Carol Ashley |
| 6 | MS 1349 | Jeffrey Brinker |
| 1 | MS 1349 | Alan Sellinger |
| 2 | MS 0750 | Randy Cygan |
| 1 | MS 0805 | Roger Assink |
| 1 | MS 0805 | Todd Alam |
| 1 | MS 1407 | Duane Dimos |
| 1 | MS 0959 | Scott Reed |
| 1 | MS 0188 | C. E. Meyers, LDRD Office |
| 1 | MS 9018 | Central Technical Files, 8940-2 |
| 2 | MS 0988 | Technical Library |
| 2 | MS 0619 | Review & Approval Desk, 12690<br>For DOE/OSTI |
| 1 | MS 0161 | Patent and Licensing Office, 11500 |